Evaluation of a dynamic multi-class sediment transport model in a catchment under soil-conservation agriculture

Peter Fiener, Gerard Govers, Kristof Van Oost

Angaben zur Veröffentlichung / Publication details:

Fiener, Peter, Gerard Govers, and Kristof Van Oost. 2008. "Evaluation of a dynamic multi-class sediment transport model in a catchment under soil-conservation agriculture." *Earth Surface Processes and Landforms* 33 (11): 1639–60. https://doi.org/10.1002/esp.1634.

Evaluation of a dynamic multi-class sediment transport model in a catchment under soil-conservation agriculture

Peter Fiener,[1]* Gerard Govers[2] and Kristof Van Oost[2]
[1]Hydrogeography and Climatology Research Group, Universität zu Köln, Cologne, Germany
[2]Physical and Regional Geography Research Group, Katholieke Universiteit Leuven, Leuven, Belgium

*Correspondence to: Peter Fiener, Department of Geography, Universität zu Köln, Albertus Magnus Platz, D-50923 Cologne, Germany. E-mail: Peter.fiener@uni-koeln.de

Abstract

Soil erosion models are essential tools for the successful implementation of effective and adapted soil conservation measures on agricultural land. Therefore, models are needed that predict sediment delivery and quality, give a good spatial representation of erosion and deposition and allow us to account for various soil conservation measures.

Here, we evaluate how well a modified version of the spatially distributed multi-class sediment transport model (MCST) simulates the effectiveness of control measures for different event sizes. We use 8 year runoff and sediment delivery data from two small agricultural watersheds (0·7 and 3·7 ha) under optimized soil conservation. The modified MCST model successfully simulates surface runoff and sediment delivery from both watersheds; one of which was dominated by sheet and the other was partly affected by rill erosion. Moreover, first results of modelling enrichment of clay in sediment delivery are promising, showing the potential of MCST to model sediment enrichment and nutrient transport.

In general, our results and those of an earlier modelling exercise in the Belgian Loess Belt indicate the potential of the MCST model to evaluate soil erosion and deposition under different agricultural land uses. As the model explicitly takes into account the dominant effects of soil-conservation agriculture, it should be successfully applicable for soil-conservation planning/evaluation in other environments.

Keywords: erosion model; sediment deposition; multi-class sediment transport; sediment delivery; soil conservation

Introduction

Soil erosion has been recognized for a long time as one of the most serious environmental problems associated with agricultural land use (Morgan, 1996). It has severe on-site as well as off-site impacts. On-site problems cover the loss of topsoil and fertilizer, the decrease in crop yield (where plants are eroded, covered by sediments or in the case of gullying) in the short term and a decrease in soil fertility in the long-term (Lal, 2001). The off-site problems, which are nowadays more in the public and political focus, are the pollution of surface waterbodies with suspended sediments and colloids (see, e.g., Haygarth *et al.*, 2006; Bilotta *et al.*, 2007) and other substances attached to the sediment particles (e.g. phosphorus and pesticides) and the silting of riverbeds, reservoirs and ponds, as well as the damage of infrastructure and private properties by local muddy floods (Verstraeten and Poesen, 1999; Boardman *et al.*, 2003).

Soil erosion and deposition models are essential tools for the implementation of effective and site-specific soil conservation measures on agricultural land. During the last decades several models have been developed. All of these models have different strengths and limitations because each was developed against the background of a particular philosophy, for different objectives and for specific site conditions (Grunwald and Frede, 1999).

Still very common is the empirical, spatially and temporally lumped Universal Soil Loss Equation (USLE, Wischmeier and Smith, 1978) and its derivates such as the Revised USLE (RUSLE, Renard *et al.*, 1991), or the Erosion-Productivity Impact Calculator (EPIC, Williams and Renard, 1985). These models assume in principle a spatially uniform slope, although they have been applied to complex terrain coupling with GIS, e.g. in the differentiated USLE (dUSLE, flacke *et al.*, 1990).

In order to improve the reliability, generality and accuracy of erosion prediction, more physical process-based erosion models have been developed within the last decades. The more recent ones are: the Water Erosion Prediction Project (WEPP, Flanagan and Nearing, 1995), the European Soil Erosion Model (EUROSEM, Morgan *et al.*, 1998), the Kinematic Runoff and Erosion Model (KINEROS2, Smith *et al.*, 1995) and the Limburg Soil Erosion Model (LISEM, De Roo *et al.*, 1996a, 1996b). Due to the complexity and the spatial and temporal variation of erosion processes a large number of parameters have been integrated in these models. Hence, much attention was paid to the acquisition of input data (Jetten *et al.*, 1996). Nevertheless, these models do not necessarily perform better than the lumped, empirical based models, mainly because input errors increase with model complexity (Jetten *et al.*, 2003) and because of uncertainties in model structure and process representation (Parsons *et al.*, 2004).

In this context, reduced complexity modelling has received increasing attention during the past few years. This tendency can be found generally in the environmental sciences and is basically due to the fact that it is now realized that better predictions might be obtained using simpler model structures with a reduced parameter space rather than very complex model systems for which the necessary parameter values and input data are impossible to obtain (see, e.g., Brazier *et al.*, 2000, 2001). Examples of such models are the Sealing Transfer Runoff Erosion Agricultural Modification model (STREAM, Cerdan *et al.*, 2001) and the Water and Tillage Erosion Model (WaTEM, Van Oost *et al.*, 2000) .

However, there exists a trade-off between reduced model complexity and the predictive power of a soil erosion model. This is especially relevant when evaluating the on- and off-site effects of different land management strategies. For this purpose, a model should (i) predict the amount as well as the size distribution of sediments delivered from an agricultural watershed, which is a major prerequisite for a reasonable prediction of the erosion and export of sediment bound substances such as particulate organic matter and nutrients, (ii) give a good spatial representation of where erosion and deposition is actually occurring at different scales, (iii) account for effects of different erosion control measures, namely changes in tillage techniques and field layout as well as the implementation of grass filter strips etc., and (iv) provide explicit information about the quality of the model predictions and the uncertainty associated with the model.

This study focuses on the dynamic Multi-Class Sediment Transport model (MCST) developed by Van Oost *et al.* (2004). Although this model uses a limited set of parameters, it is dynamic and accounts for size-selectivity during sedimentation, within a two-dimensional context on an event basis. Erosion patterns, sediment delivery and sediment quality can therefore be modelled. Thus far the model has only been tested for rainfall-runoff events in a small conventionally managed watershed (3·0 ha) in the loam belt of Belgium, where measured erosion and deposition patterns after a series of winter storms were used for model validation (Van Oost *et al.*, 2004). To use the model under different environmental conditions, especially to account for soil conservation techniques, more rigorous model testing and possibly model modifications are necessary.

Our objectives were (i) to validate the MCST model using a unique 8 year monitoring data set from two small watersheds (0·7 and 3·7 ha) managed using optimized soil conservation techniques, located in Southern Germany, (ii) to modify the model in terms of process representation in order to simulate adequately soil erosion processes under soil conservation and (iii) to carry out first tests of the modified model's ability to predict grain size distribution in delivered sediments, a prerequisite to simulate the transport of sediment bound substances.

Materials and Methods

Study site

The study site is part of the Scheyern Experimental Farm located about 40 km north of Munich in the Tertiary hills, an important agricultural landscape in Central Europe. The study site covered two small adjacent agricultural watersheds 3·7 and 0·7 ha in size (Figure 1), situated at an altitude of 454–469 m above sea level (48°30′50″ North, 11°26′30″ East). Loamy and silty loamy Inceptisols dominate throughout the watershed (Sinowski and Auerswald, 1999), with a median grain size diameter between 12·5 and 16 μm. Between 1994 and 2001 the mean annual air temperature was 8·4 °C, and the mean annual soil temperature at a depth of 0·05 m under grass was 10·2 °C. Ground frost was observed approximately 21 days per year occurring between December and the beginning of March. The average annual precipitation (1994–2001) was 834 mm.

Both watersheds drained a single large field with a crop rotation consisting of potato (*Solanum tuberosum* L.), winter wheat (*Triticum aestivum* L.), maize (*Zea mays* L.) and winter wheat. Before each row crop a cover crop (mustard, *Sinapis alba* L.) was cultivated after wheat harvest in August. Potato ridges were already formed prior to mustard seeding and potatoes and maize were planted directly into the winter-frost killed mustard, maintaining some

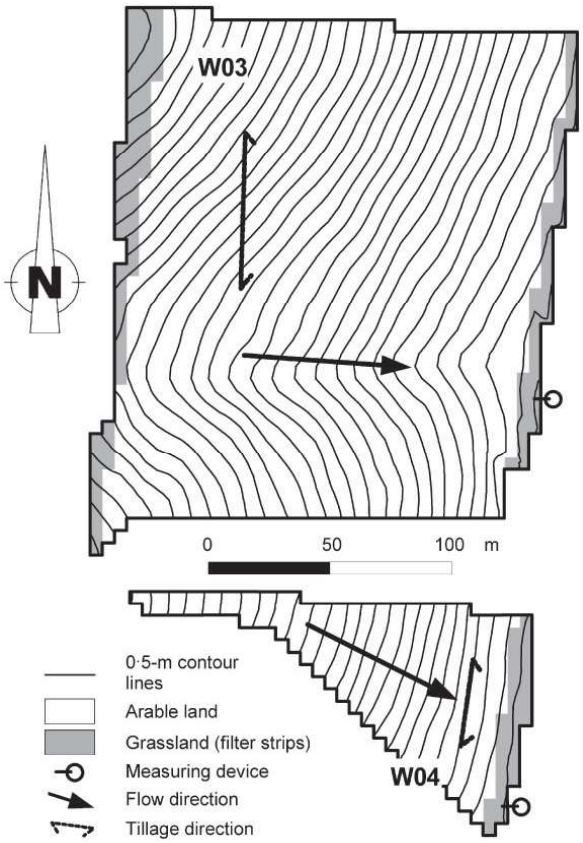

Figure 1. Topography, field borders, tillage direction and location of measuring devices in watersheds W03 and W04.

mustard cover after planting the potatoes. Wide low-pressure tires were used on all machinery to reduce soil compaction and to avoid the development of wheel-track depressions, which usually encourage runoff (Auerswald *et al.*, 2000; Fiener and Auerswald, 2003b). At the down-slope end of the field in both watersheds a 5–10 m wide vegetated filter strip (VFS) was established, wherein the runoff is routed along a slightly elevated field road to the watershed outlet (Figure 1).

Data collection

Runoff was continuously collected between 1994 and 2001 at the outlet of the watersheds. The measuring systems were based on a Coshocton-type wheel runoff sampler collecting an aliquot of 0·52–0·55% (watersheds W03 and W04, respectively) from the total runoff coming from the outflow pipe. The aliquot volume was measured and at least one sample was taken during or after each event, and later dried at 105 °C to determine the sediment concentration. The measuring system was tested for function at the end of each runoff event. A more detailed description of the measuring system and the results of a precision test can be found in the work of Fiener and Auerswald (2003a).

Two meteorological stations were located about 500 and 100 m from the watersheds at 453 and 480 m above sea level, respectively. At these stations triggered rainfall data (0·2 mm per trigger) were collected. For modelling, the measurements were aggregated to minute values and the data of the farther station were only used in the case of equipment failure of the nearer station. Precipitation events were differentiated when no rainfall was measured for at least 6 h.

Plant and residue cover was measured bi-weekly during the vegetation period, four weekly in autumn and spring, and before and after each soil management operation. The measurements were carried out at three locations in the field of the tested watersheds and in three neighbouring fields with identical crop rotation between January 1993 and April 1997. Residue cover was measured manually using a pocket rule. Plant height was determined in the field and plant cover was derived from photographs taken around noon from a height up to 4 m (in the case of full-grown maize) using image analysis. Therefore, photographs were digitized and the percentage of plant cover was calculated after interactively determining all areas with and without plant cover. Between January 1994 and April 1997 the cover

measurements made in the watershed were directly used for modelling. From May 1997 to December 2001 an average cover of each specific crop was derived from all measurements (including measurements in neighbouring fields) covering 16 years of winter wheat and 8 years of maize and potato, respectively. This average cover information was adjusted to account for field operations, which were all monitored during the total measuring campaign (1994–2001).

Soil samples were taken in a 50 m × 50 m grid in both watersheds to derive soil properties, such as grain size distribution, carbon and nutrient content etc. For model parameterization we used the grain size distribution in the topsoil (0–0·2 m) homogenized by field operations. To determine grain size distribution the topsoil samples were dispersed, decalcified and analysed with the sieve–pipette method.

Modelling Structure

A detailed description of the MCST model was given by Van Oost *et al.* (2004). Here, we give an overview of the most important components and focus on the modifications made in this study. MCST is a grid based model and has three major components: (i) a runoff generation module using a modified SCS curve number (CN) technique, (ii) a runoff routing algorithm that redistributes runoff via flow paths to the outlet of a watershed taking into account flow direction effects due to tillage roughness and (iii) an erosion, transport and deposition module calculating the spatial distribution of soil erosion and deposition.

Runoff generation. The runoff generation routine in the original MCST was only tested for wet winter conditions under conventional agriculture (Van Oost *et al.*, 2004). To apply the model for different seasons under conservation agriculture, the originally used SCS curve number technique was fundamentally modified to account for variations of antecedent soil moisture, effects of cover management, soil crusting, run-on and infiltration after the end of rain event (afterflow infiltration) in areas of high infiltration capacities.

In the original SCS CN model the antecedent soil moisture content (AMC) is taken into account for three different soil moisture conditions (dry, average and wet) represented by different equations to calculate the CNs (see, e.g., Chow *et al.*, 1988). The incorporation in terms of three AMC levels causes unreasonable and sudden jumps in the CN variation. To prevent these and to objectify the simulation, an approach developed by Mishra *et al.* (2004) was adopted. In this approach, which was tested for about 63 000 storm events from 234 watersheds in the USA varying in size from 0·1 ha to 30 350 ha, runoff generation is calculated taking the five days antecedent precipitation AP_5 into account:

$$R_{CN} = \frac{(P - I_a)(P - I_a + M)}{P - I_a + M + S} \tag{1}$$

$$I_a = \lambda S \tag{2}$$

$$M = 0{\cdot}5\left[-(1 + \lambda)S + \sqrt{(1 - \lambda)^2 S^2 + 4AP_5\, S}\right] \tag{3}$$

where R_{CN} is the estimated direct surface runoff (mm), S is the potential maximum retention (mm), I_a is the initial abstraction (mm), P is the total precipitation of an event (mm), M is the antecedent soil moisture (mm) and AP_5 is the antecedent 5 day precipitation amount (mm).

In the original curve number technique, time is not represented and hence the technique does not allow accounting for variations in rainfall intensity and duration. Van Oost (2003) found that using Equation (4) to account for rainfall intensity significantly improved the prediction of direct runoff from a small agricultural watershed in the Belgium loam belt, so this was also implemented.

$$R = R_{CN}(IN_{max10}/10)^{\alpha} \tag{4}$$

where IN_{max10} is the maximum 10 minute rainfall intensity and α is a calibration parameter.

Furthermore, to use the curve number technique in small agricultural watersheds under different cropping practices the selection of CNs used to calculate S should follow objective rules accounting for surface conditions, namely soil cover and crusting stage. To represent the effect of soil cover on CNs an approach presented by Auerswald and Haider (1996) was adopted. These authors found in plot experiments (plot size 7–187 m^2, 1 h rain of 60–74 mm, SCS-CN hydrological soil group C) carried out at the Scheyern test site and in the surrounding landscape that there is a more distinct difference between CNs for different field conditions than represented by the original approach (e.g. USDA-SCS, 1986). In general the experiments demonstrated a strong relationship between soil cover by plants and plant residues and CN. For small grains this is described by Equation (5) (Auerswald and Haider, 1996), while for row crops Equation (6) can be used (Auerswald, 2002).

$$CN_{SG} = 87 - 47COVER \qquad (n = 51,\ R = -0{\cdot}91) \tag{5}$$

$$CN_{RC} = 80 - 40COVER \qquad (n = 23,\ R = -0{\cdot}77) \tag{6}$$

where COVER represents relative soil cover (plants and plant residues), CN_{SG} and CN_{RC} are CNs for small grains and row crops, respectively, and the standard error for the Pearson correlation coefficient R is 0·06 and 0·13 for Equations (5) and (6), respectively; for both equations R is significantly different from zero ($P < 0{\cdot}001$).

The plot experiments were carried out under uncrusted conditions (personal communication, K. Auerswald) and, hence, crusting was introduced following Equation (7) (Van Oost, 2003):

$$CN = CN_{SG/RC} + \frac{1}{5}CRc \tag{7}$$

where CR is the crusting stage (Govers, 1986), $CN_{SG/RC}$ are CNs derived from Equations (5) and (6) and c is a crusting coefficient.

The crusting stages vary between 0 and 5, representing the full range from a non-sealed, initial fragmentary structure with all fragments clearly distinguishable to a continuous state with depositional crusts (Govers, 1986). The value of c is set so that the CN for crusting stage 5 is equal to the CN of 0% soil cover according to Equations (5) and (6) (for small grains $c = 87 - CN_{SG}$; for row crops $c = 80 - CN_{RC}$). The introduction of crusting stages into the CN calculations was successfully applied for a small agricultural watershed in the Belgium Loam Belt, where crusting stages were monitored over three years (Van Oost, 2003).

To ensure the applicability of the model where such measurements are not available, we introduced and modified a soil crusting approach developed by Schröder and Auerswald (2000; Schröder, 2000). The principal ideas of this approach are the following: (i) Following Morin and Benyamini (1977), the decrease in infiltration rate caused by soil crusting can be described by a negative exponential equation taking into account start and minimum (end) infiltration rate, rainfall energy and a parameter representing soil susceptibility to crusting. (ii) If the soil is protected by a plant or a residue cover, the effective rainfall energy is reduced and hence the soil is less vulnerable to crusting. (iii) The initial infiltration rate for an event following a crusting event is equal to the end infiltration rate of the preceding event. (iv) During a period without rain there is a decay of the existing crust caused by earthworm activity and soil crack formation. Due to the complex interaction of soil properties (texture, organic carbon content, pH etc.) and earthworm activity as well as soil temperature and moisture the authors did not find any adequate physical basis to calculate the time of recovery. Therefore, a simple estimate, is used applying a crust half-life time of 30 days approximated from field experience.

For our approach we modified the original exponential equation, introducing crusting stages instead of start and minimum infiltration rates:

$$CR(t_1) = CR_{max} - (CR_{max} - CR(t_0))e^{-C_B Ekin_{eff}(t_1)} \tag{8}$$

where $CR(t_1)$ is the crusting stage after time t_1, $CR(t_0)$ is crusting at the beginning of the event, CR_{max} is equal to crusting stage 5, and $Ekin_{eff}$ is the effective kinetic rain energy.

$$Ekin_{eff} = \int_{t_0}^{t_1} Ekin(t)(1 - COVER)\,dt \tag{9}$$

where Ekin is the energy of a rainfall for time t, and t_0 is the start time of a rain event.

Kinetic rainfall energy Ekin is calculated following the standard USLE procedure (Wischmeier and Smith, 1958) also applied under German conditions (Schwertmann *et al.*, 1987). For 53 rainfall experiments at the Scheyern research farm carried out on plots under seedbed conditions with a wide range of soil textures (plots of 8 m^2, 1 h rain of 60–63 mm, slope 1–14%, clay content 12–31%, silt content 15–67%), Schröder and Auerswald (2000) found that a kinetic rainfall energy of about 400–500 J m^{-2} produced a fully crusted soil, a result that is in line with other experiments on loamy and clay soils (see, e.g., Lado *et al.*, 2004). Further rainfall experiments with different soil covers ($n = 39$, cover 10–25%) allowed us to confirm that the relationship between crusting and rainfall kinetic energy can also be used for surfaces covered with vegetation residue provided that the effective kinetic rain energy reaching the soil surface, $Ekin_{eff}$, is used.

The soil crusting parameter C_B was determined based on the 53 rainfall experiments under seedbed conditions, where the start and minimum infiltration rate (crusting stage 0 and 5, respectively) were measured and rainfall kinetic

energy was calculated from measured rain intensities. C_B was most strongly related to soil texture: for soils of texture class 1, i.e. soils with a clay content between 15 and 22%, the average C_B is 0·015 (SD 0·007, $n = 19$). For soils of texture class 2, characterized by a silt content less than 50%, the average C_B was 0·0075 (SD = 0·005, $n = 34$).

To approximate the recovery of crusting stages (or infiltration rates) Equation (10) was used. Moreover, crusting stage was set to zero in the case of any tillage operation.

$$\mathrm{CR}(t_0, n) = \mathrm{CR}(t_{\mathrm{end}}, n-1) - \mathrm{CR}(t_{\mathrm{end}}, n-1)(1 - e^{\mathrm{fr}\Delta t}) \tag{10}$$

where $\mathrm{CR}(t_0, n)$ is the crusting stage at the beginning of a new event, $\mathrm{CR}(t_{\mathrm{end}}, n-1)$ is the crusting stage at the end of the previous event, fr is a recovery parameter, and Δt is the time of crust recovery. Due to a lack of clear information on the factors controlling crust recovery, a simple time dependency is used, where fr was set to –0·02 to reach a half-life time of the crust of 30 days.

Runoff routing. In the MCST model a numerical solution of the kinematic wave approximation is used to estimate discharge and water depth at every location in the grid at all time steps. MCST uses different hydrological models for sheet flow and concentrated (rill) flow. Sheet flow is modelled according to the Manning equation and it is assumed that the flow width is equal to the grid cell size. For self-forming rills, flow velocities and cross-sectional areas are predicted from discharge alone (Govers, 1992b). Moreover, the model uses a multiple-flow algorithm for sheet flow, while a single-flow algorithm is used for rills.

The model assumes sheet flow until a critical shear stress of 0·9 Pa is exceeded, which is sufficient to initiate rill formation on an erodible loamy soil (Govers, 1985). In this study, shear stress was calculated as

$$\tau = \rho g D S \left(\frac{n_g}{n}\right)^{3/2} \tag{11}$$

where τ is shear stress (Pa), ρ is water density (kg m^{-3}), g is the acceleration due to gravity (m s^{-2}), D is the flow depth (m), S is the local slope, n_g is the Manning roughness coefficient for bare soil and n is the Manning roughness coefficient depending on plant and plant residue cover.

Compared to the original MCST the term $(n_g/n)^{3/2}$ in Equation (11) was added to the general shear stress calculation to account for the reduced shear stress affecting the soil surface if the soil is protected by plant residues (Govers, 1992a). This situation can typically be found under soil conservation agriculture or if soil is covered by dense grass due to the installation of vegetated filter strips (VFSs). The Manning roughness coefficients for surfaces covered with plant residues are calculated following Gilley *et al.* (1991). From flume experiments (flow rates $5{\cdot}24 \times 10^{-4}$–$1{\cdot}01 \times 10^{-1}$ m^3 s^{-1}) these authors derived empirical relationships between different types of plant residue (cover 15–99%) and Manning's n. For Reynolds numbers less than 20 000 Equation (12) can be used for different residues types:

$$n = 1{\cdot}89 \times 10^{-2}(\mathrm{COVER_R})^{0{\cdot}712}/\mathrm{Re}^{0{\cdot}142} \tag{12}$$

where $\mathrm{COVER_R}$ is surface cover by plant residues, and Re is Reynolds number.

For the calculation of Manning's n in the model a Reynolds number of 2000 was used. For Watershed W03 typical values calculated for Re range between 250 and 2000. Hence, the Re used to calculate n leads in most cases to a conservative estimate of the hydraulic roughness effect of soil cover introduced by soil conservation. Clearly, this correction procedure could be improved if more information on runoff hydraulics on vegetation covered surfaces were available.

To decide whether runoff will follow the topographical or the tillage direction, the TCRP model of Takken *et al.* (2001) is used. They found that runoff patterns on agricultural land are strongly affected by tillage direction. Incorporation of these effects in runoff routing significantly improved prediction of erosion and deposition patterns.

To allow for run-on and afterflow infiltration, which can both be prominent in the case of soil conservation measures such as grassed waterways, simple estimates of these infiltration rates derived from the CN methodology are used in the modified MCST. If runoff is routed into a grid cell where no rain excess occurs till time t, re-infiltration I_{RE} (mm s^{-1}) is calculated and the initial abstraction of this cell is reduced by the re-infiltrated volume:

$$I_{\mathrm{RE}}(t) = \frac{(I_a - P)D_d}{D_s} \tag{13}$$

where P is the cumulative precipitation (mm) till time t, D_d is the event duration in days (–) used to scale I_a and P, and D_s is the event duration (s).

Afterflow infiltration is assumed if runoff is routed through a grid cell that previously produced infiltration excess. This is especially important for areas along the thalwegs of a watershed, where runoff lasts longest after the end of a precipitation event, and where conservation measures can effectively reduce runoff velocity due to an increased hydraulic roughness. This afterflow infiltration I_{AF} (mm s^{-1}) is estimated using Equation (14):

$$I_{AF}(t) = I_{cum}/D_s \tag{14}$$

where I_{cum} is the cumulative infiltration (mm) during an event according to the SCS-CN methodology ($I_{cum} = S(P - I_a)/(P - I_a + S)$).

Based on the dynamic simulation of rainfall, infiltration and runoff generation, the MCST model calculates an effective steady-state flow and effective runoff duration.

Erosion, transport and deposition. The erosion, transport and deposition component of the MCST model uses a concept of three different erosion/deposition domains, representing areas dominated by different erosion/deposition processes as proposed by Beuselinck *et al.* (1999a, Figure 2). Below a critical threshold, no entrainment of particles occurs and sediment deposition is governed by simple settling as a function of fall velocity (Domain 1). Above this threshold, two other domains were identified, where entrainment of original soil, deposition and re-entrainment of the deposited particles all occur simultaneously. In Domain 3 entrainment and re-entrainment are dominant, resulting in net erosion, while in Domain 2 deposition is dominant but significant sediment re-entrainment occurs.

The concept was implemented in the MCST model of Van Oost *et al.* (2004) and was successful in predicting the erosion/deposition pattern in a small agricultural watershed (3 ha) in the Belgium loam belt after a wet winter (1992–1993). Under these conditions (conventional cultivation of winter wheat with a cover less than 10%, erosion prone silty loam) erosion/deposition is dominated by rill erosion in areas where $\Omega > \Omega_{cr}$ and deposition of the rill-eroded sediment at the foot slope: it was therefore not necessary to explicitly account for sediment transport by interrill runoff. To predict soil erosion during the vegetation period under soil conservation agriculture, sheet erosion, driven by a combination of rain drop impact and flow transport, must be explicitly taken into account. Therefore, we modified the process description for Domain 1 (Figure 2).

It is generally accepted that soil detachment by splash far exceeds the transporting capacity of interrill flow, so that interrill erosion is basically a transport-limited process (Foster and Meyer, 1975). Interrill transporting capacity was modelled using the interrill transporting capacity relationships developed by Everaert (1991). Based on a series of flume experiments with typical interrill flow discharges (unit discharge: 0·002–0·025 $m^2\ m^{-1}\ s^{-1}$), Everaert developed transporting capacity relationships. On slopes ranging from 1·7 to 17·4%, without and with rain on the surface (intensity of 60 mm h^{-1}), the solid discharge in the case of a median sediment diameter between 33 and 122 μm can be expressed as

$$q_s = 1{\cdot}74 \times 10^{-6} \Omega_{cff}^{1{\cdot}07} D_{50}^{0{\cdot}47} \qquad (R^2 = 0{\cdot}89;\ n = 394) \tag{15}$$

and the effective stream power is calculated as (Govers, 1990; Foster and Meyer, 1972)

$$\Omega_{cff} = \Omega^{3/2} D^{-2/3} \tag{16}$$

where Ω is stream power (g s^{-3}) and D is flow depth (cm).

Equation (15) is used to model interrill sediment transport in Domain 1. If the sediment input into a raster cell is larger than its specific potential to transport solid discharge, size-selective deposition is assumed. Therefore, ten

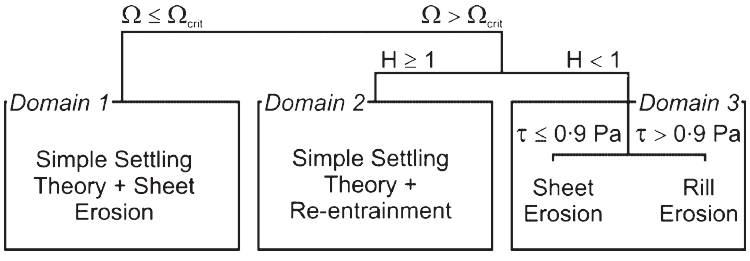

Figure 2. General implementation scheme of modified dynamic Multi-Class Sediment Transport model (MCST).

equally distributed sediment classes represented by specific settling velocity classes are used and continuous mixing of water and sediment is assumed (Beuselinck *et al.*, 1999a). Sediment concentration c_i for each settling velocity class is given by (Beuselinck *et al.*, 1999b; Hairsine *et al.*, 2002)

$$c_i(x) = c_{i0}\mathrm{e}^{\frac{-v_i x_i}{q}}, \qquad i = 1, 2, \ldots I - 1 \tag{17}$$

where c_{i0} is the initial concentration of velocity class c_i, v_i is the settling velocity of class i and x_i is the evaluation distance.

In contrast to the approach used to model sediment re-entrainment (Domains 2 and 3), changes in grain size distribution due to selective deposition are not taken into account to calculate interrill sediment transport in Domain 1.

Erosion and deposition in Domains 2 and 3 are calculated according to the original MCST model (Van Oost *et al.*, 2004). If the local stream power exceeds Ω_{cr}, the shielding factor H, from the Hairsine–Rose model (1992a, 1992b), is calculated to decide whether net deposition (Domain 2) or net erosion (Domain 3) occurs:

$$H = \frac{(\sigma - \rho)g\sum v_i c_i}{\sigma F(\Omega - \Omega_{\mathrm{cr}})} \tag{18}$$

where σ is sediment density (kg m^{-3}), ρ water density (kg m^{-3}) and F the fraction of stream power used for re-entrainment. As H is a shielding factor, its maximum value is set to $H = 1$.

If $H = 1$ (Domain 2), simultaneous re-entrainment and deposition of sediment occurs. The variation of sediment concentration with distance downslope can then be described as follows for steady-state flow (Sander *et al.*, 2002):

$$\frac{\mathrm{d}c_{\mathrm{r}}}{\mathrm{d}x} = \left[\frac{\gamma^*}{\sum_{i=1}^{I} v_i c_i} - 1\right]\frac{v_i c_i}{q}, \qquad i = 1, 2, \ldots I \tag{19}$$

where

$$\gamma^* = \gamma q^{1-\frac{1}{m}}\left[1 - \frac{\Omega_{\mathrm{cr}}}{\Omega}\right], \tag{20}$$

$$\gamma = \frac{F\sigma\rho S K^{\frac{1}{m}}}{\sigma - \rho} \tag{21}$$

and the flow depth D is given by the generalized depth discharge equation

$$D = \left(\frac{q}{K}\right)^{\frac{1}{m}} \tag{22}$$

where q is the unit discharge (m^2 s^{-1}) and K is a coefficient related to surface slope and hydraulic roughness ($K = S^{1/2}/n$), and m is a flow constant of 5/3 for turbulent flow (Beuselinck *et al.*, 2002).

From these equations the spatial pattern of sediment deposition and sorting of all sediment size classes can be calculated if values for c_i, v_i, q, S, D and σ are known at the entry and the exit of each grid cell.

If $H < 1$, net erosion occurs (Domain 3). As long as the flow shear stress (Equation (11)) is below the critical value for rill initiation of 0·9 Pa, interrill erosion is modelled according to Equation (15). If τ exceeds the critical value, rill detachment is calculated as a function of slope and discharge following Equation (23):

$$\mathrm{Dr} = a_{\mathrm{rill}} S^{\mathrm{ser}} Q^{\mathrm{de}} \tag{23}$$

where Dr is the detachment rate (kg m^{-1} s^{-1}), a_{rill} is a rill erodibility factor, S is the local slope gradient, Q is the rill discharge and ser and de are topographical exponents, which are based on rill erosion experiments conducted by Gimenez and Govers (2002), and are set to fixed values of ser = 0·9 and de = 0·73 (Govers *et al.*, 2007).

Table I. Main input data, parameters and variables of the Multi-Class Sediment Transport model (MCST)

Description	Symbol	Unit	Range/value
Digital terrain model		m	5 × 5
Land use map			
Soil cover for each field and land use		%	0–100
Tillage roughness (and direction) for each field	R_o	m	0–0·25
Hydraulic roughness fields	n	s m$^{-1/3}$	0·016–0·300
Water density	ρ	kg m^{-3}	1000
Sediment density	σ	kg m^{-3}	1800–2600
Vertical mixing coefficient		/	1
Characteristic settling velocity for class i	v_i	m s^{-1}	1.6×10^{-7}–$3{\cdot}4 \times 10^{-2}$
Threshold of re-entrainment	τ_{cr}	Pa	0·6
Threshold of rill erosion		Pa	0·9
Re-entrainment parameter	F	/	0·1
Hydraulic roughness vegetated filter strip	n_{UFS}	s m$^{-1/3}$	0·20
Curve number	CN	/	65

Model implementation

To simulate runoff formation and routing in the runoff module a precalibration procedure, using nine runoff events (>0·5 mm) in Watershed W03, was applied to determine the parameters λ and α, accounting for antecedent soil moisture (Equation (3)) and rain intensity (Equation (4)), as well as a_{rill} to consider the site-specific rill erodibility (Equation (23)). The optimal parameter set was determined using the highest model efficiency coefficient (MEF), as proposed by Nash and Sutcliffe (1970).

$$\text{MEF}_i = 1 - \frac{\sum_{i=1}^{n}(Q_i - M_i)^2}{\sum_{i=1}^{n}(O_i - \overline{O})^2} \tag{24}$$

where O_i is the observed and M_i is the modelled variable of parameter set i.

The main input data required for the model, except for the calibration parameters given in the results section, are summarized in Table I. Moreover, ten equally distributed sediment size classes for each watershed were calculated from the soil sampling at the test site. The time step used for modelling was 60 s.

The output of the model consists of the following maps: discharge of every time step, effective discharge, stream power, location of sheet and rill erosion, net erosion/deposition and deposition of each sediment size class. Moreover, a hydrograph, total runoff, total sediment output and sediment size distribution at the outlet are also calculated.

Results and Discussion

Measurements

During the observation period (1994–2001) 1413 rainfall events have resulted in 218 and 154 runoff and sediment delivery events in Watersheds W03 and W04, respectively. On average a runoff of 38·5 mm a^{-1} (runoff coefficient 0·05) and a sediment delivery of 437 kg ha^{-1} a^{-1} were measured in W03 during the 8 year observation, while in W04 measured average annual runoff was 9·6 mm a^{-1} (runoff coefficient 0·01) and sediment delivery was 40 kg ha^{-1} a^{-1} (Figure 3). The difference in runoff coefficient by a factor of five was probably caused by a different area ratio between field and vegetated filter strip (the VFS–field area ratio is equal to 1/28 and 1/8 in W03 and W04, respectively). The area and topography also play an important role in sediment production and delivery: W03 has a much higher total sediment yield because this watershed has longer and partly steeper slopes and a clearly defined thalweg, which is more prone to rill erosion. The formation of rills was observed in W03 after a few larger events, while almost no rills developed in W04.

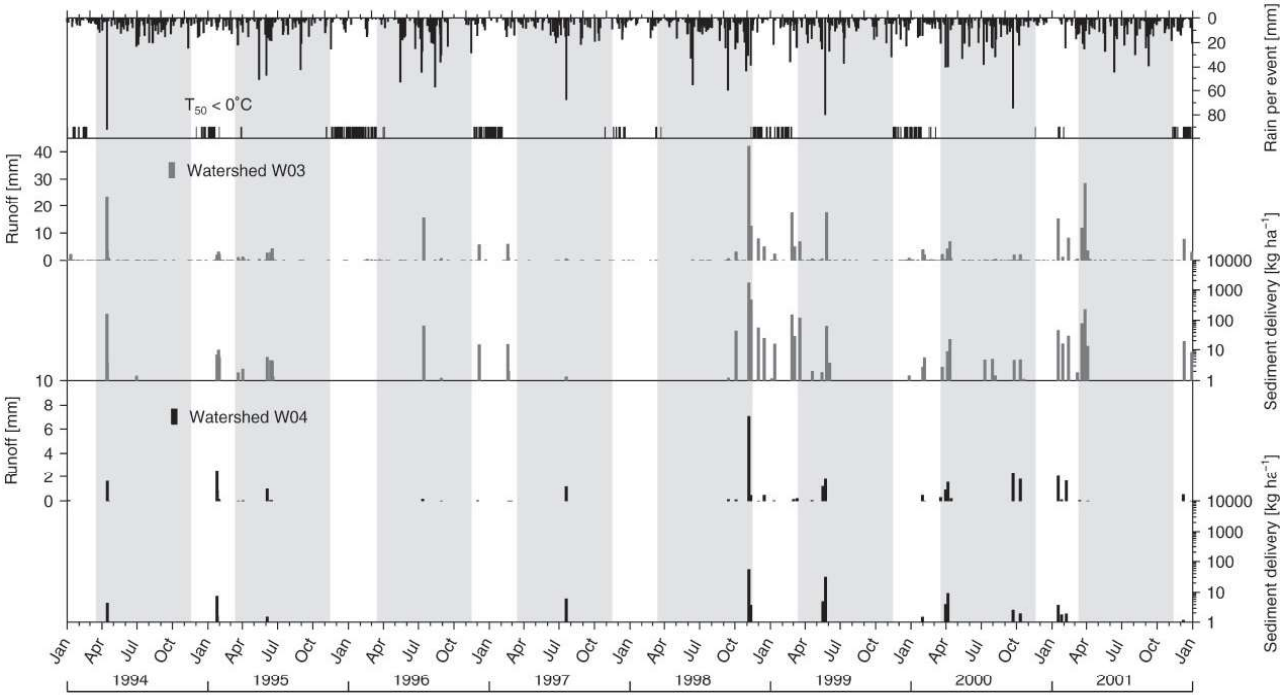

Figure 3. Measured rainfall, runoff, sediment delivery and air temperature below 0 °C (1994–2001) at the tested watersheds in Scheyern; only those events are shown where runoff from Watershed W03 is at least 0·5 mm; grey bars indicate time periods (April–November) used for modelling as long as the air temperature was above 0 °C.

The relatively low rates of soil erosion and runoff are attributed to the soil conservation techniques established in the watersheds, which result in a high soil cover by plants and plant residues throughout the year (Figure 4) (Auerswald and Haider, 1996; Auerswald *et al.*, 2000; Fiener and Auerswald, 2001). Hence, during the vegetation period (April–November), when the highest rain intensities can be expected (see, e.g., Bartels *et al.*, 1997), only a few storms produce significant runoff volumes (>0·5 mm). Nevertheless, these storms dominate the erosion (72% of the total annual sediment delivery) within this period; two large erosion events contributed substantially to the total sediment delivery in Watershed W03. These events, occurring within two weeks after potato harvest in October 1998 (Figure 3), produced a sediment delivery of 1715 and 467 kg ha^{-1}, respectively, representing 61·5% of total sediment delivery measured within the 8 year observation period. In contrast, relatively low sediment delivery rates were observed in W04, which drains the same large field as W03: here only 55 and 4 kg ha^{-1} was measured for the same events, which again can be attributed to a shorter slope length and hence absence of intensive rill formation and a wider vegetated filter strip at the down-slope end of the watershed.

Modelling

The MCST model is not able to represent snow melt or ground frost, and events where these processes played an important role were excluded from our analysis. For the test site snow and ground frost free conditions are met for the period from April to November (Figure 3). During the 8 year observation 108 and 92 events occurred between April and November in W03 and W04, respectively, representing 86 and 84% of the total measured sediment delivery.

For practical reasons, and due to the fact that only the largest events dominate the erosion processes, only those events with a runoff in Watershed W03 of at least 0·5 mm were modelled. The selected events represent 95·5% of runoff and 98·7% of sediment delivery measured in W03 between April and November (1994–2001). For Watershed W04 the same events were modelled, to evaluate whether the model has the ability to handle more rill erosion driven events in W03 as well as interrill dominated events in W04. An overview of all modelled events and the associated event and watershed characteristics is given in Table II.

Hydrology. The precalibration procedure of the hydrology module to determine the optimal parameter set for λ and α, accounting for antecedent soil moisture and rain intensity, showed that the model is highly sensitive to changes in

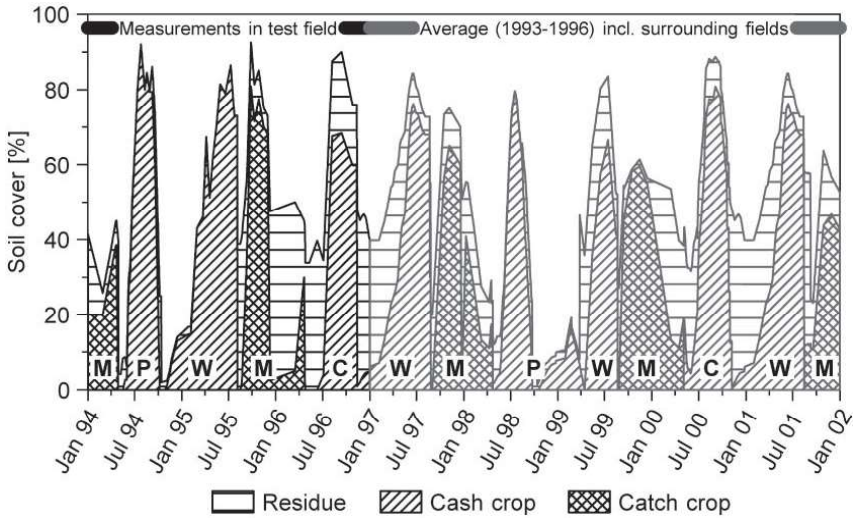

Figure 4. Averaged field soil cover derived from measurements within the field drained by watersheds W03 and W04 and from three surrounding fields with an identical crop rotation and similar soils; Between 1994 and 1996 the measurements within the test field were used; From 1997 to 2001 the soil cover was derived from the average cover measurements (1994–1996) in the test field and in the three neighbouring fields, taking into account the individual field operations within the test field occurring 1997 to 2001 (W = wheat, C = maize, P = potato, M = mustard).

λ, while changes in α have only a minor effect as long as λ is close to the optimal value (Figure 5). An optimal model performance for the nine calibration events (Table II) indicated by an MEF of 0·88 and an RMSE of 3·2 mm could be obtained using a λ of 0·2 and an α of 0·7. The calibration results in exactly the standard λ value used in the original SCS-CN approach. From Figure 5 it is obvious that the calibrated value of α gives a very similar model efficiency to the one that could be reached using an α of 0·9 obtained by Van Oost (2003) through a similar calibration procedure for a Belgian watershed.

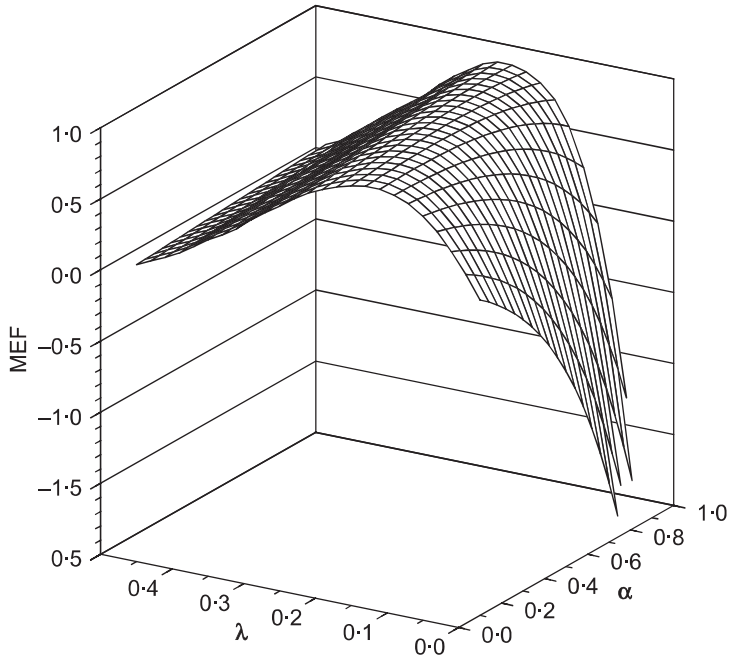

Figure 5. Model efficiency (MEF) calculated according to Nash and Sutcliffe (1970) for the hydrological module of MCST, varying the calibration parameters λ and α, accounting for antecedent soil moisture (Equation (3)) and rain intensity (Equation (4)).

Table II. Precipitation and field characteristics, measured and modelled runoff and sediment delivery, for all runoff events in Watershed W03 ≥ 0.5 mm; P_{tot} is the total precipitation of an event; I_{max10} is the maximum 10-minute rain intensity, AR5 is the 5-days antecedent rain; $Q_{obs/mod}$ is the observed and modelled runoff; $SD_{obs/mod}$ is the observed and modelled sediment delivery; *CN* and *n* field is the curve number and the Manning *n* within the field located in both watersheds

		Precipitation characteristics				Watershed W03					Watershed W04					Field conditions in W03 and W04		
Date	No. Event	Ptot [mm]	Imax10 [mm/h]	Duration [h]	AR5 [mm]	Qobs [mm]	Qmod [mm]	SDobs [kg/ha]	SDmod [kg/ha]	Calibration data = 0; validation data = 1	Qobs [mm]	Qmod [mm]	SDobs [kg/ha]	SDmod [kg/ha]	Calibration data = 0; validation data = 1	Tillage roughness [cm]	*CN* Field	*n* Field
04/12/1994	100	86·8	8·4	38·8	9·4	27·0	32·0	161·9	134·5	0	–[+]	–	–	–	–	25	82	0·024
04/16/1994	101	2·4	1·2	9·5	88	0·9	0·0	0·2	0·0	0	0·00	0·00	0·00	0·00	1	25	85	0·024
03/21/1995	137	23·2	3·6	49·0	12	1·0	0·0	1·8	0·0	1	0·04	0·00	0·18	0·00	1	2	78	0·016
04/02/1995	141	11·8	2·4	33·0	11·2	1·6	0·0	3·3	0·0	1	0·01	0·00	0·06	0·00	1	2	81	0·016
06/02/1995	147	49·0	7·2	24·7	18·2	2·7	5·8	5·8	42·4	1	0·98	3·13	1·49	7·70	1	2	72	0·016
06/13/1995	149	18·2	6	23·5	17·4	2·9	0·2	4·5	10·7	1	0·04	0·00	0·18	0·00	1	2	83	0·016
06/15/1995	150	20·4	16·8	11·2	21·2	4·3	1·4	4·4	36·9	0	0·04	0·00	0·16	0·00	1	2	86	0·016
06/19/1995	151	8·4	4·8	25·8	24	0·5	0·0	1·4	0·0	1	0·01	0·00	0·03	0·00	1	2	81	0·016
07/05/1996	175	73·6	9·6	67·1	11·8	15·5	9·5	65·4	71·1	0	0·14	3·27	0·64	14·03	1	5	79	0·071
08/28/1996	178	30·4	9·6	16·3	59·2	0·7	1·9	1·2	15·7	0	0·00	0·00	0·00	0·00	1	5	76	0·056
09/11/1998	222	60·6	7·2	43·2	8·6	0·7	3·2	1·2	23·3	0	0·12	0·00	0·20	0·00	1	25	72	0·021
09/29/1998	224	42·6	9·6	125·5	10·6	3·1	3·1	44·4	31·3	0	0·09	0·00	0·26	0·00	1	0	88	0·016
10/29/1998	228	107·4	13·2	156·1	45·6	42·1	34·5	1714·9	761·4	1	7·03	5·56	54·92	58·66	1	0	87	0·016
11/09/1998	229	38·6	4·8	155·6	16·2	12·6	5·8	467·4	58·2	1	0·46	0·00	3·79	0·00	1	0	87	0·016
04/19/1999	247	26·4	4·8	88·6	9·2	0·5	0·0	2·0	0·0	1	0·05	0·00	0·53	0·00	1	2	84	0·092
05/14/1999	252	25·6	31·2	27·0	27·2	0·5	0·0	1·8	0·0	0	1·18	0·00	4·98	0·00	1	2	68	0·051
05/21/1999	253	80·6	8·4	62·8	0·2	17·5	13·9	64·5	74·4	0	1·79	10·69	31·08	18·27	1	2	69	0·046
09/22/2000	309	74·8	12	39·2	12·4	2·0	12·3	4·5	67·1	1	2·33	10·31	2·46	16·21	1	5	66	0·029
10/07/2000	311	30·8	4·8	47·1	22·6	2·1	0·0	4·7	0·0	1	1·79	0·00	1·88	0·00	1	5	70	0·029

[+] no measurements due to equipment failure.

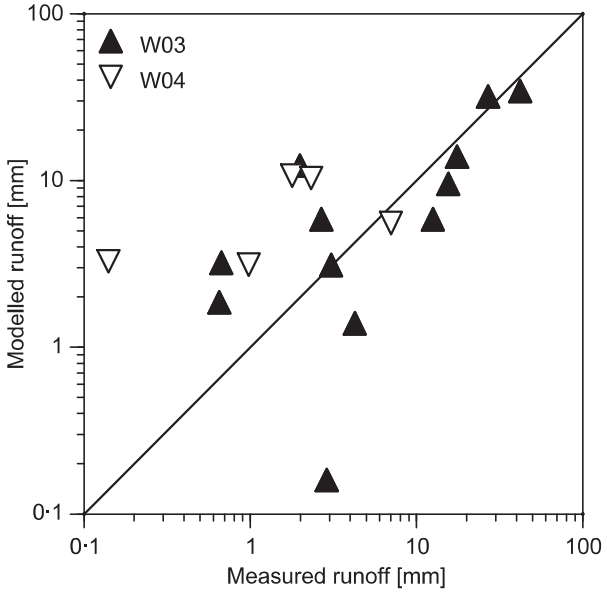

Figure 6. Measured versus modelled runoff in Watersheds W03 and W04 for measured runoff events in Watershed W03 of at least 0·5 mm.

Based on the standard model parameterization (Table I) and the calibrated values of λ and α, the comparison of measured and predicted runoff volumes for all 19 events in Watershed W03 larger than 0·5 mm shows a reasonable model performance (MEF = 0·86, RMSE = 4·1 mm). This is especially true for the larger events dominating the overall erosion during the observation period (Table II, Figure 6). For smaller events (measured runoff <3 mm) the modified MCST model partly overestimated runoff, and for some events no runoff was simulated while a runoff between 0·5 and 2·1 mm (average = 1·0 mm) was observed. This indicates that for small storms it is problematic to use a static value of λ to determine the initial abstraction or rainfall amount that must be reached before rain excess occurs. This problem has already been reported by Hawkins *et al.* (1985): they concluded that the standard CN method should only be used for storm depths of at least 0·46 times the maximum retention depth for average moisture conditions.

Comparing measured and predicted runoff volumes for all 18 events in Watershed W04, in general a much weaker model performance (MEF = –2·3, RMSE = 3·0 mm) was determined. This might have three main reasons: (i) the runoff module was calibrated for W03; (ii) in W04 the observed runoff volumes (maximum 7·0 mm, Table II) were generally smaller and therefore higher errors can be expected due to the increasing event variance with decreasing event size (see, e.g., Nearing, 2006); (iii) as the observed runoff volumes in W04 vary only between 0 and 47 m^3, while in W03 volumes from 20 to 1550 m^3 were measured, the relative runoff reduction effect of the downslope VFS in both watersheds is more pronounced in the smaller Watershed W04. Hence, the model results are in general much more sensitive to parameterization and size of the VFS. This is shown for Event 253 (Figure 7, Table II). The simulation of the effects of such small structures is difficult due to a lack of data on their temporally variable properties (see, e.g., Fiener and Auerswald, 2006), the unknown degree of concentration of runoff within these structures and a potentially too coarse spatial resolution, which does not account for the exact size and geometry of the VFS. Due to these problems the analysis of erosion and deposition modelling is focused on the larger runoff events dominating the overall erosion in both watersheds. For these larger events the overall performance of the runoff module, indicated by an overall MEF in both watersheds of 0·82 and a RMSE of 3·6, is assumed to be sufficient.

Erosion and Deposition. As more important erosion events occurred in Watershed W03, the data from this watershed are mainly used to evaluate the erosion–deposition component of the model. Nevertheless, the erosion and deposition modelling is also tested against data from W04 to evaluate whether the model predicts the occurrence of rills correctly.

Based on effective discharge and effective event duration, the patterns of erosion and deposition as well as sediment delivery from the watersheds were modelled.

As there are no data from rill erosion experiments using soils from the research farm in Scheyern, the erosion module has to be calibrated to determine the rill erodibility coefficient a_{rill}. Best results for the nine calibration events were reached for a rill erodibility coefficient of 46 (MEF = 0·88, RMSE = 17·7 kg ha^{-1}).

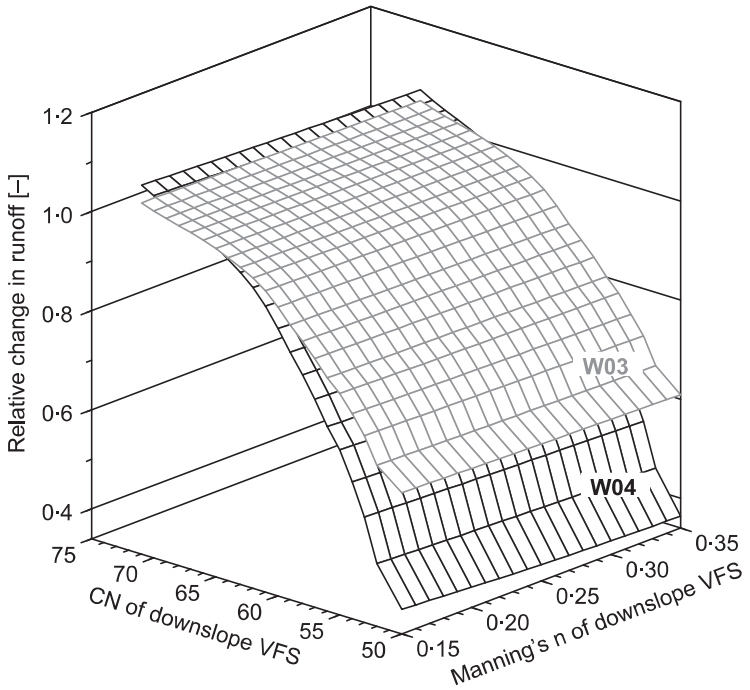

Figure 7. Relative change in modelled runoff volume for Event 253, comparing the results of the standard parameterization of the vegetated filter strips (VFSs) located at the down-slope end of Watersheds W03 and W04 with results from varying Manning's *n* and curve number (CN) for the VFSs; standard parameterization for the VFSs is $n_{VFS} = 0{\cdot}2$ and $CN_{VFS} = 65$ (Table I).

Based on the calibration, a comparison between measured and modelled sediment delivery is shown in Figure 8. The generally smaller sediment delivery per watershed area in Watershed W04 compared with W03 is well represented by the model. Nevertheless, sediment delivery from W04 is overestimated for all events less than 2·5 kg ha^{-1}, again indicating problems with runoff prediction for these small events. This represents a general problem in model accuracy in the case of watersheds under soil conservation. As event size decreases due to conservation measures, the

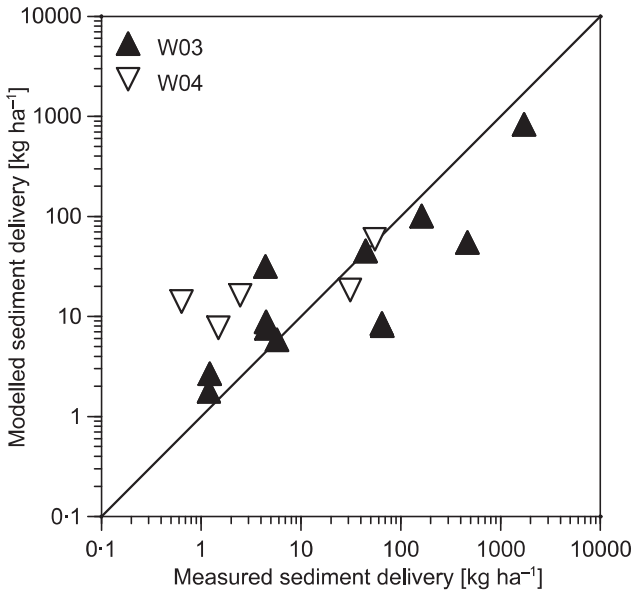

Figure 8. Measured versus modelled sediment delivery in Watersheds W03 and W04 for measured runoff events in Watershed W03 of at least 0·5 mm.

Table III. Range of results for modelled effective discharge (Q_{eff}), sediment delivery and spatial proportion of erosion/deposition domains, as well as total sediment delivery ratio (SDR_{tot}) for watersheds W03 and W04

	Watershed W03			Watershed W04		
	Max.	**Min.**	**Average**	**Max.**	**Min.**	**Average**
Q_{eff} outlet ($m^3 s^{-1}$)	0·0243	0·00	0·0088	0·0035	0·00	0·0016
Sediment delivery (kg ha^{-1})	761·4	0·0	69·8	58·7	0·0	6·4
Area of watershed[+] in						
Domain 1 (%)	100·0	82·1	98·4	100·0	93·7	99·1
Domain 2 (%)	0·5	0·0	0·1	0·0	0·0	0·0
Domain 3 (%)	17·3	0·0	1·5	6·3	0·0	0·8
Proportion of deposition[+] in						
Domain 1 (%)	100·0	38·5	77·0	100·0	100·0	100·0
Domain 2 (%)	61·5	0·0	23·0	0·0	0·0	0·0
SDR_{total}[+]	0·52	0·15	0·34	0·29	0·15	0·22

[+] Results given for all events where a runoff greater than 0·0 was modelled.

variance in sediment delivery of single events increases, which was shown by Nearing *et al.* (1999) for more than 2000 natural rainfall events on erosion plots distributed all over the United States.

For the largest event (No. 228, Table II), the modelled effective discharge in W03 was about seven times larger than in W04 (Table III), while the modelled sediment delivery differs by a factor of about 13. While in Watershed W04 almost no linear erosion in rills was predicted (Figures 9 and 10) and no rills were documented by a qualitative observation, the erosion in the larger Watershed W03 was dominated by rill erosion, which was modelled (Figures 9 and 10) and also qualitatively observed after the event. Nevertheless, in W03 the sediment delivery for this largest event, representing 67% of total sediment delivery, was significantly underestimated. In the case of Event 228 a heavy rain ($P = 107$ mm; $I_{max10} = 13{\cdot}2$ mm h^{-1}) fell on an erosion prone field shortly after potato harvest. Due to field operations during harvest the soil had almost no cover (<2%) and the soil was in a very erodible condition as it was sieved by the potato harvester, thereby decreasing the stable aggregate diameter (e.g. a D_{50} of 120 and 55 µm was measured before and after harvest in 1995) (Fiener and Auerswald, 2007). Moreover, the VFS at the downslope end of the watershed was partly damaged due to repeated crossing with the potato harvester.

Under these specific conditions, the model underestimates the sediment delivery by a factor of 2·3, which is probably caused by the static parameterization of soil and VFS properties. The difficulties in predicting erosion and deposition accurately in the case of Event 228 are a major reason for the relatively low MEF of 0·62 and high RMSE of 238 kg ha^{-1} for the erosion model validation, because both measures of goodness of fit are highly sensitive to the largest values of a comparison. The situation in the case of Event 228, especially the part failure of the VFS, also points out a general problem in the parameterization of erosion models under very specific conditions, which are not properly monitored even at a research farm. This is even more problematic for optimized soil conservation systems, where larger events are rarer compared to conventional agriculture, and where these events more often occur in the case of a part failure of the conservation system, which is difficult to parameterize.

Considering the fact that soil erosion is an inherently variable phenomenon (e.g. Nearing, 1998), we may conclude that the MCST model yields promising results for conservation tillage. Nevertheless, further analysis of model uncertainties and further tests under different land management conditions must be carried out for an ongoing improvement of the model.

Rill erosion was qualitatively observed by regular field visits during the observation period (1994–2001), therefore the modelled rill erosion after large events along the thalweg of W03 and the near absence of rills in W04 could be confirmed. Moreover, as expected, modelled sedimentation in the VFS at the downslope end of the watersheds was indeed found in the field after the larger events.

Focusing on the model representation of the processes in the different domains (Figure 2, Table III), most areas in both watersheds belong to Domain 1, representing sheet erosion and simple settling (average area in W03 and W04 98·4 and 99·1% respectively). This indicates that in both watersheds sheet erosion is the dominant process during most events. Only for the larger events in W03 are Domains 2 and 3 more prominent (maximum 17·3 and 0·5%, respectively). Despite the small area of the field experiencing re-entrainment (Domain 2), Domain 2 can dominate total deposition in W03 in the case of large events (Table III) and its explicit consideration may therefore improve

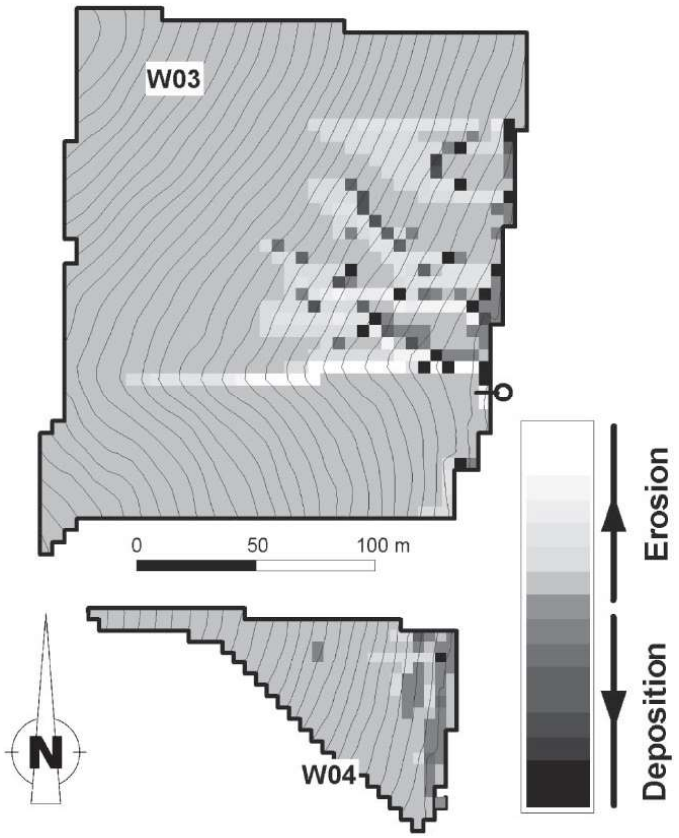

Figure 9. Spatially distributed modelling of erosion and deposition in watersheds W03 and W04 for Event 228 occurring at the beginning of October 1998.

modelling of sediment size-selective erosion and deposition in a watershed experiencing significant erosion. Re-entrainment in Domain 2 was not modelled for any of the 18 events in W04.

Due to the fact that no detailed field surveys of changes in topsoil texture after erosion events were made, which would have been more or less impossible because of the small erosion and deposition amount under the soil conservation system, it is not possible to compare measured and modelled patterns of clay, silt or sand enrichment within the watersheds. However, the enrichment of clay and organic matter in sediments leaving the watersheds was measured in all 16 watersheds (including the test watersheds) of the Scheyern research farm in 1993 and 1994. From these data Auerswald and Weigand (1999) derived a relationship between enrichment of fines, total sediment delivery of an event and median texture in a watershed:

$$\log(\mathrm{ER}) = -0{\cdot}27 + 0{\cdot}45 \log(D_{50}) - 0{\cdot}05 \log(\mathrm{SD}) \qquad (R^2 = 0{\cdot}51,\ n = 195) \qquad (25)$$

where ER is the enrichment of clay and organic matter (–), D_{50} is the median grain size (μm) of a watershed and SD is the sediment delivery (t ha^{-1}).

As Equation (25) was derived from the tested watersheds and 14 others of similar scale (0·5–16 ha), we assume that it is reasonable to compare the results from Equation (25) with the clay enrichment modelled by MCST (Figure 11). For total clay delivery the modelled clay enrichment fits very well with the results of the Auerswald–Weigand (1999) approach. This is a first indication that MCST is able to predict clay enrichment in delivered sediments. As the enrichment of sediment bound nutrients and organic matter is often closely related to the enrichment of clay in delivered sediments (see, e.g., Auerswald and Weigand, 1999; Steegen *et al.*, 2001), MCST also has, therefore, the potential to predict nutrient or organic matter delivery.

Representation of soil conservation agriculture. One of the main goals of this study was to test whether the MCST model can adequately represent soil erosion and deposition under conservation agriculture. Therefore, the main aspects of soil conservation in fields, namely permanent soil cover, adapted crop rotation and minimum mechanical soil disturbance, as well as structural measures such as reducing field sizes, VFS or grassed waterways, were taken into account.

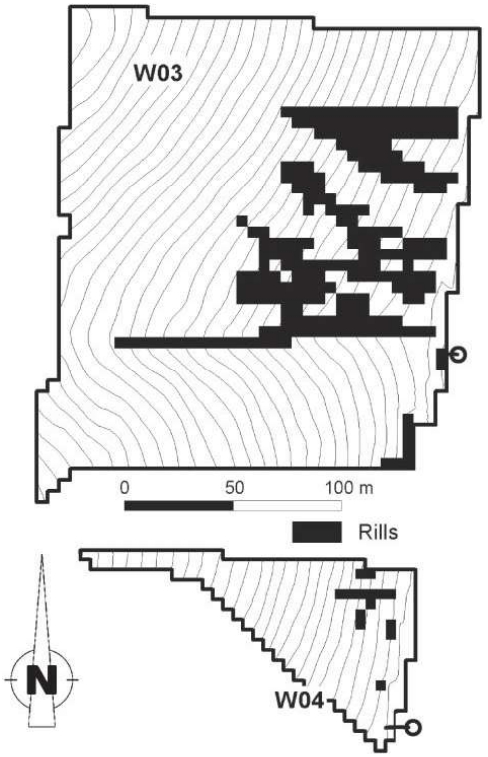

Figure 10. Modelled rill pattern in watersheds W03 and W04 for Event 228 occurring at the beginning of October 1998.

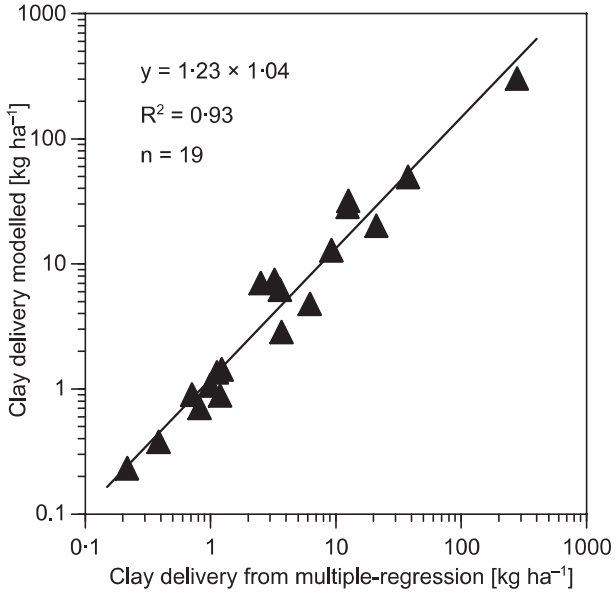

Figure 11. Comparison between clay delivery calculated with a multiple-regression approach (Auerswald and Weigand, 1999) using modelled total sediment delivery and median sediment size in Watersheds W03 and W04 (Equation (25)) and the clay delivery due to the sediment size-selective modelling presented in this study.

The aspects of cover management and adopted crop rotation are considered in MCST, as soil cover is one of the dominant parameters in the model. It affects (i) runoff formation, which was intensively tested in rainfall experiments (Schröder and Auerswald, 2000; Auerswald and Haider, 1996) used to modify the traditional CN technique, (ii) runoff velocity, because of its dependence on hydraulic roughness and the decision between interrill and rill flow, (iii) peak

Table IV. Modelled effect of soil residue cover on curve number and hydraulic roughness (Manning's *n*), and hence on runoff volume, peak discharge and volume of afterflow infiltration, shown for 86·8 mm rain occurring on 12–14 April 1994 in Watershed W03; for the calculations a constant plant cover of 20% is assumed

Residue cover [%]	Curve number	Manning's *n*	Runoff volume		Peak discharge		Afterflow infiltration	
			[m^3]	[%]	[$m^3\ s^{-1}$]	[%]	[m^3]	[%]
0	85	0·016	1350	100	0·063	100	73	5
10	84	0·031	1282	95	0·056	89	90	7
20	82	0·045	1166	86	0·049	78	101	9
30	80	0·057	1061	79	0·043	69	106	10
40	77	0·068	913	68	0·036	57	106	12
50	73	0·079	727	54	0·027	43	103	14

discharge, which is reduced when runoff velocity decreases, and (iv) afterflow infiltration, which increases with decreasing runoff velocity. All these aspects have a strong impact on modelled runoff volume and peak discharge; this is illustrated for a range of surface covers in the case of Event 100 occurring in April 1994 (Table IV). For example, if the surface residue cover increases from 0 to 50% a decrease in runoff volume of 46% and in peak discharge of 57% is modelled.

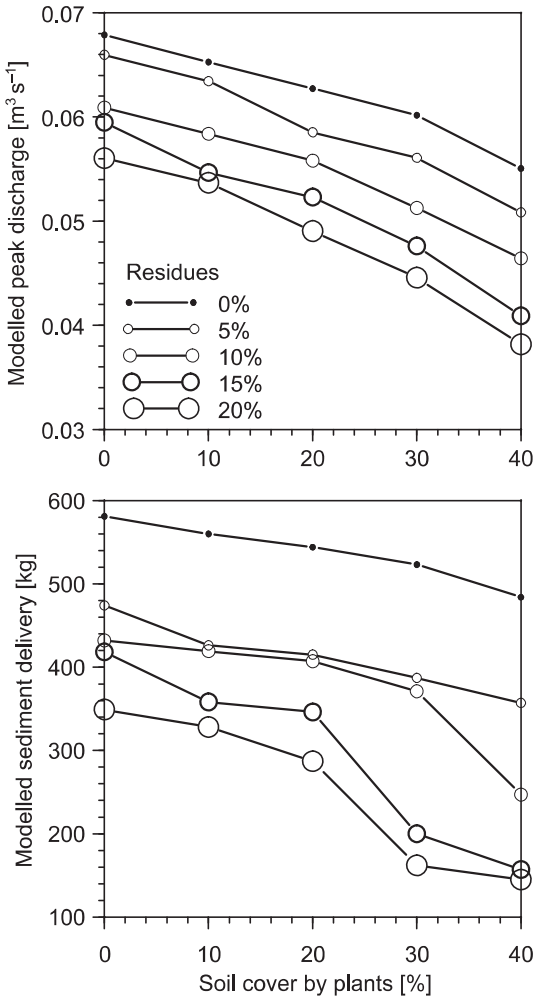

Figure 12. Effects of changes in soil cover by plants and plant residues on modelled peak discharge and sediment delivery, exemplarily shown for Event 100, which occurred in April 1994 (Table II).

While modelled peak discharge is more or less linearly related to plant and plant residue cover, modelled sediment delivery is not (Figure 12). For example, if residue cover in the case of Event 100 increases from 0 to 5% (10% plant cover), the total sediment delivery decreases by 24% (134 kg) because no rills are modelled at the downslope end of the thalweg of W03. Hence, sediments are deposited instead of being delivered to the outlet. This indicates that the model is sensitive to slight changes in cover management, which can reduce total sediment delivery significantly. This was indeed the case for W03, where, in an 8 year observation period, rills were most likely to occur in the case of total cover failure (e.g. Event 228) and almost no rills have been observed as long as a small surface cover could be maintained.

In addition to the representation of soil cover, the MCST model also allows simulation of soil conservation measures such as VFS or grassed waterways. By taking into account their high hydraulic roughness and infiltration capacity, the calculation of runoff velocity, run-on, afterflow infiltration, transport capacity and erodibility is modified. Minimum mechanical disturbance is only indirectly represented in the model by taking residue cover into account and by using a site-specific rill erodibility factor. The static parameterizations of site-specific soil properties inhibit the representation of seasonal or inter annual variations and long-term changes in soil structure. This can be problematic in the case of rare specific soil conditions, e.g. the case of the largest erosion event during the 8 year observation period (Event 228, Figure 8), where the soil was strongly disturbed and disaggregated after potato harvest.

The importance of low frequency, high magnitude events becomes higher under conservation agriculture than under conventional agriculture as they occur only in the relatively short periods when the soil is unprotected, e.g. after potato harvest and damage of the VFS in Watershed W03. Moreover, these rare events are often the result of site-specific conditions, which are extremely difficult to represent, e.g. the partial failure of the VFS in W03 in the case of Event 228.

One of the incentives to develop and test MCST was that erosion models often need a large number of parameters for which data are often not available. While MCST also still needs a considerable number of parameter values, model behaviour is still transparent as the role of the various parameters can be easily understood. An advantage of the model is also that many of its modules are based on existing model structures so that an estimate of most parameter values needed can be obtained from available literature, at least for silty loam soils. Its dynamic, 2D nature nevertheless implies that MCST is primarily aimed at applications in a research environment.

Conclusions

The monitoring of runoff, sediment delivery and watershed characteristics clearly show that optimized soil conservation minimizes soil loss. Nevertheless, even under optimal soil conservation practices, soil protection is insufficient during short periods, e.g. shortly after potato harvest in the case of the largest measured event, and large erosion and deposition events may occur. As these events are rarer compared to conventional agriculture, data sets covering longer periods of time are required to evaluate the erosion potential of a soil conservation system and to test the performance of models. The 8 year data record used in this study provided a comprehensive basis for model testing and modification.

In this study a modified version of the MCST model was used. To consider soil conservation measures in the watersheds, effects of soil cover on runoff formation, runoff routing, run-on and afterflow infiltration as well as rill erosion were taken into account. Moreover, algorithms for interrill erosion, more prominent under soil conservation, where rills can be widely prevented, were implemented.

Application of this modified MCST model indicated that in the case of runoff events greater than 3 mm the model simulated runoff accurately, while for small events results are biased by the threshold behaviour of the modified SCS-curve number technique and probably also by the dominant effects of runoff conservation structures such as VFS, which are difficult to parameterize. As the larger events dominate the erosion and deposition within the watersheds, the overall results of the runoff module are promising. Moreover, the relatively simple model structure and the calibration results for λ and α (Figure 5), which indicate that the modelled runoff is only slightly sensitive to α and the value of λ can be set to the SCS-CN standard value, warrant a wider applicability.

The model also showed reasonable results for sediment delivery (MEF = 0·62; $n = 37$), and for larger events modelled interrill, rill and sedimentation patterns were confirmed by qualitative field observations. In most cases, soil conservation measurements were adequately represented in the model by taking into account the effects on soil plant and plant residue cover. In principle, the model is easy to use in other watersheds under soil conservation, where soil cover data can be estimated. However, better data on rill erodibility may be necessary as well as a better approach to predict the effect of vegetation cover on runoff hydraulics, as it was recently shown that the approach developed by Gilley *et al.* (1991) may not always be applicable (Giménez and Govers, 2008).

The application also demonstrated some fundamental limitations to the modelling of single events: single events may play a very important role but characterization of the causative rare and site-specific soil conditions leading to high erosion rates can be extremely difficult.

The sediment size-specific modelling of deposition successfully reproduced the clay enrichment at the watershed outlet as proposed by a regression model developed at the research farm (Auerswald and Weigand, 1999). As such, the model is one of the first 2D models to have the ability to dynamically model the delivery of sediment bound substances to watercourses. The fact that space can be represented correctly in the model is essential: tillage direction as well as the presence of soil conservation structures cannot be accounted for when a 1D hillslope profile approach is used.

Acknowledgements

The scientific activities of the research network 'Forschungsverbund Agrarökosysteme München' (FAM) were financially supported by the German Federal Ministry of Education and Research (BMBF 0339370). The Bavarian State Ministry for Science, Research and Arts funded overhead costs of the research station. The modelling was done in the framework of a post-doctoral fellowship at the K.U. Leuven, Belgium. The authors would like to thank all members of the FAM project contributing to the manuscript with fruitful discussion and/or the collection of data sets used here; special thanks goes to Karl Auerswald, who initiated and stimulated the erosion research in Scheyern and beyond.

References

Auerswald K. 2002. Landnutzung und Hochwasser. In *Katastrophe oder Chance? Hochwasser und Ökologie*. Pfeil, Monich; 67–76.

Auerswald K, Albrecht H, Kainz M, Pfadenhauer J. 2000. Principles of sustainable land-use systems developed and evaluated by the Munich Research Alliance on agro-ecosystems (FAM). *Petermanns Geographische Mitteilungen* **144**: 16–25.

Auerswald K, Haider J. 1996. Runoff curve numbers for small grain under German cropping conditions. *Journal of Environmental Management* **47**: 223–228.

Auerswald K, Weigand S. 1999. Eintrag und Freisetzung von P durch Erosionsmaterial in Oberflächengewässern [Input and detachment of phosphorus caused by sediments in surface water bodies]. *VDLUFA-Schriftenreihe* **50**: 37–54 (in German).

Bartels H, Malitz G, Asmus S, Albrecht FM, Dietzer B, Günther T, Ertel H. 1997. *Starkniederschlaghöhen für Deutschland – KOSTRA* [*Recurrence Time of Rain Intensities – KOSTRA*]. Deutscher Wetterdienst: Offenbach am Main (in German).

Beuselinck L, Govers G, Steegen A, Hairsine PB, Poesen J. 1999a. Evaluation of the simple settling theory for predicting sediment deposition by overland flow. *Earth Surface Processes and Landforms* **24**: 993–1007.

Beuselinck L, Govers G, Steegen A, Quine TA. 1999b. Sediment transport by overland flow over an area of net deposition. *Hydrological Processes* **13**: 2769–2782.

Beuselinck L, Hairsine PB, Sander GC, Govers G. 2002. Evaluating a multiclass net deposition equation in overland flow conditions. *Water Resources Research* **38**: 10.1029/2001WR000248.

Bilotta GS, Brazier RE, Haygarth PM. 2007. Processes affecting transfer of sediment and colloids, with associated phosphorus, from intensively farmed grasslands: erosion. *Hydrological Processes* **21**: 135–139.

Boardman J, Evans R, Ford J. 2003. Muddy floods on the South Downs, southern England: problems and responses. *Environmental Science and Policy* **6**: 69–83.

Brazier RE, Beven K, Anthony S, Rowan JS, Quinn P. 2001. Implications of complex model uncertainty for the mapping of hillslope scale soil erosion predictions. *Earth Surface Processes and Landforms* **26**: 1333–1352.

Brazier RE, Beven KJ, Freer J, Rowan JS. 2000. Equifinality and uncertainty in physically based soil erosion models: application of the glue methodology to WEPP – the Water Erosion Prediction Project – for sites in the UK and USA. *Earth Surface Processes and Landforms* **25**: 825–845.

Cerdan O, Souchere V, Lecomte V, Couturier A, Le Bissonnais Y. 2001. Incorporating soil surface crusting processes in an expert-based runoff and erosion model STREAM (Sealing Transfer Runoff Erosion Agricultural Modification). *Catena* **46**: 189–205.

Chow VT, Maidment DR, Mays LW. 1988. *Applied Hydrology*. McGraw-Hill: New York.

De Roo AP, Offermans RJE, Cremers HDT. 1996a. LISEM: a single-event, physically based hydrological and soil erosion model for drainage basins. II: Sensitivity analysis, validation and application. *Hydrological Processes* **10**: 1119–1126.

De Roo AP, Wesseling CG, Ritsema CJ. 1996b. LISEM: a single-event physically based hydrological and soil erosion model for drainage basins. I: Theory, input and output. *Hydrological Processes* **10**: 1107–1117.

Everaert W. 1991. Empirical relations for the sediment transport capacity of interril flow. *Earth Surface Processes and Landforms* **16**: 513–532.

Fiener P, Auerswald K. 2001. Eight years of economical and ecological experience with soil-conserving land use. In *Multidisciplinary Approaches to Soil Conservation Strategies*, Helming K (ed.). Zentrum für Agrarlandschafts und Landnutzungsforschung (ZALF), Müncheberg; 121–126.

Fiener P, Auerswald K. 2003a. Effectiveness of grassed waterways in reducing runoff and sediment delivery from agricultural watersheds. *Journal of Environmental Quality* **32**: 927–936.

Fiener P, Auerswald K. 2003b. Concept and effects of a multi-purpose grassed waterway. *Soil Use and Management* **19**: 65–72.
Fiener P, Auerswald K. 2006. Seasonal variation of grassed waterway effectiveness in reducing runoff and sediment delivery from agricultural watersheds in temperate Europe. *Soil and Tillage Research* **87**: 48–58.
Fiener P, Auerswald K. 2007. Rotation effects of potato, maize and winter wheat on soil erosion by water. *Soil Science Society of America Journal* **71**: 1919–1925.
Flacke W, Auerswald K, Neufang L. 1990. Combining a modified Universal Soil Loss Equation with a digital terrain model for computing high resolution maps of soil loss resulting from rain wash. *Catena* **17**: 383–397.
Flanagan DC, Nearing MA. 1995. *USDA Water Erosion Prediction Project: Hillslope Profile and Watershed Model Documentation*, National Soil Erosion Research Laboratory Report 10. USDA-ARS NSERL: West Lafayette.
Foster GR, Meyer LD. 1972. Transport of soil particles by shallow flow. *Transactions of the American Society of Agricultural Engineers* **15**: 99–102.
Foster GR, Meyer LD. 1975. Mathematical simulation of upland erosion by fundamental erosion mechanics. In *Present and Prospective Technology for Predicting Sediment Yields and Sources,* ARS-S-40. USDA Science and Education Administration; 190–204.
Gilley JE, Kottwitz ER, Wieman GA. 1991. Roughness coefficients for selected residue materials. *Journal of Irrigation and Drainage Engineering – American Society of Civil Engineers* **117**: 503–514.
Gimenez R, Govers G. 2002. flow detachment by concentrated flow on smooth and irregular beds. *Soil Science Society of America Journal* **66**: 1475–1483.
Giménez R, Govers G. 2008. Short term effects of incorporated straw residue on rill erosion and hydraulics. *Catena* **72**: 214–223.
Govers G. 1985. Selectivity and transport capacity of thin flows in relation to rill erosion. *Catena* **12**: 35–49.
Govers G. 1986. *Soil Erosion Process Research: a State of the Art*, Academiae Analecta 58(1). Mededelingen van de Koniklijke Academie voor Wetenschappen, Letteren en Schone Konsten van België: Brussels.
Govers G. 1990. Empirical relationships for the transport capacity of overland flow. In *Proceedings of the Jerusalem Workshop 1987*, Jerusalem; 45–63.
Govers G. 1992a. Evaluation of transporting capacity formulae for overland flow. In *Overland flow – Hydraulics and Erosion Mechanics*, Parsons AJ, Abrahams AD (eds). UCL Press: London; 243–271.
Govers G. 1992b. Relationship between discharge, velocity and flow area for rills eroding loose, non-layered materials. *Earth Surface Processes and Landforms* **17**: 515–528.
Govers G, Giménez R, Van Oost K. 2007. Rill erosion: exploring the relationship between experiments, modelling and field observations. *Earth-Science Reviews* **84**: 87–102.
Grunwald S, Frede H-G. 1999. Using the modified agricultural non-point source pollution model in German watersheds. *Catena* **37**: 319–328.
Hairsine PB, Beuselinck L, Sander GC. 2002. Sediment transport through an area of net deposition. *Water Resources Research* **38**: Art. No. 1086 JUN.
Hairsine PB, Rose CW. 1992a. Modeling water erosion due to overland flow using physical principles. 1. Sheet flow. *Water Resources Research* **28**: 237–243.
Hairsine PB, Rose CW. 1992b. Modeling water erosion due to overland flow using physical principles. 2. Rill flow. *Water Resources Research* **28**: 245–250.
Hawkins RH, Hjelmfeldt AT, Zevenbergen AW. 1985. Runoff probability, storm depth, and curve numbers. *Journal of Irrigation and Drainage Engineering – American Society of Civil Engineers* **111**: 330–340.
Haygarth PM, Bilotta GS, Bol R, Brazier RE, Butler PJ, Freer J, Gimbert LJ, Granger SJ, Krueger T, Macleod CJA, Naden P, Old G, Quinton JN, Smith B, Worsfold P. 2006. Processes affecting transfer of sediment and colloids, with associated phosphorus, from intensively farmed grasslands: an overview of key issues. *Hydrological Processes* **20**: 4407–4413.
Jetten V, Boiffin J, De Roo AP. 1996. Defining monitoring strategies for runoff and erosion studies in agricultural catchments: a simulation approach. *European Journal of Soil Science* **47**: 579–592.
Jetten V, Govers G, Hessel R. 2003. Erosion models: quality of spatial predictions. *Hydrological Processes* **17**: 877–900.
Lado M, Ben-Hur M, Shainberg I. 2004. Soil wetting and texture effects on aggregate stability, seal formation, and erosion. *Soil Science Society of America Journal* **68**: 1992–1999.
Lal R. 2001. Soil degradation by erosion. *Land Degradation and Development* **12**: 519–539.
Mishra SK, Jain MK, Singh VP. 2004. Evaluation of the SCS-CN-based model incorporating antecedent moisture. *Water Resources Management* **18**: 567–589.
Morgan RPC. 1996. *Soil Erosion and Conservation*. Addison-Wesley: Reading, MA.
Morgan RPC, Quinton JN, Smith RE, Govers G, Poesen JWA, Auerswald K, Chisci G, Torri D, Styczen ME. 1998. The European soil erosion model (EUROSEM): a dynamic approach for predicting sediment transport from fields and small catchments. *Earth Surface Processes and Landforms* **23**: 527–544.
Morin J, Benyamini Y. 1977. Rainfall infiltration into bare soils. *Water Resources Research* **13**: 813–817.
Nash JE, Sutcliffe JV. 1970. River flow forecasting through conceptual models: part I. A discussion of principles. *Journal of Hydrology* **10**: 282–290.
Nearing MA. 1998. Why soil erosion models over-predict small soil losses and under-predict large soil losses. *Catena* **32**: 15–22.
Nearing MA. 2006. Can soil erosion be predicted? In *Soil Erosion and Sediment Redistribution in River Catchments: Measurement, Modelling and Management*, Owens PN, Collins AL (eds). CABI Publishing: Wallingford; 145–152.
Nearing MA, Govers G, Norton DL. 1999. Variability in soil erosion data from replicated plots. *Soil Science Society of America Journal* **63**: 1829–1835.

Parsons AJ, Wainwright J, Powell DM, Brazier RE. 2004. A conceptual model for determining soil erosion by water. *Earth Surface Processes and Landforms* **29**: 1293–1302.

Renard KG, Foster GR, Weesies GA, Porter JP. 1991. RUSLE – Revised Universal Soil Loss Equation. *Journal of Soil and Water Conservation* **46**: 30–33.

Sander GC, Hairsine PB, Beuselinck L, Govers G. 2002. Steady state sediment transport through an area of net deposition: multi-size class solutions. *Water Resources Research* **38**: 1087. DOI: 10.1029/2001 WR000323

Schröder R. 2000. *Modellierung von Verschlämmung und Infiltration in landwirtschaftlich genutzten Einzugsgebieten* [*Modelling Silting and Infiltration in Agricultural Watersheds*], PhD thesis, Universität Bonn (in German).

Schröder R, Auerswald K. 2000. Modellierung des Jahresgangs der verschlämmungsinduzierten Abflussbildung in kleinen landwirtschaftlich genutzten Einzugsgebieten [Modelling the seasonal variation of silting induced runoff generation in small agricultural watersheds]. *Zeitschrift für Kulturtechnik und Landentwicklung* **41**: 167–172 (in German).

Schwertmann U, Vogl W, Kainz M. 1987. *Bodenerosion durch Wasser – Vorhersage des Abtrags und Bewertung von Gegenmaßnahmen* [*Soil Erosion by Water – Prediction of Soil Loss and Valuation of Counter-Measures*]. Ulmer: Stuttgart (in German).

Sinowski W, Auerswald K. 1999. Using relief parameters in a discriminant analysis to stratify geological areas with different spatial variability of soil properties. *Geoderma* **89**: 113–128.

Smith RE, Goodrich DC, Woolhiser DA, Unkrich CL. 1995. KINEROS – a kinematic runoff and erosion model. In *Computer Models of Watershed Hydrology*, Singh VP (ed.). Water Resources Publications: Collins, USA; 697–732.

Steegen A, Govers G, Takken I, Nachtergaele J, Poesen J, Merckx R. 2001. Factors controlling sediment and phosphorus export from two Belgian agricultural catchments. *Journal of Environmental Quality* **30**: 1249–1258.

Takken I, Govers G, Steegen A, Nachtergaele J, Guerif J. 2001. The prediction of runoff flow directions on tilled fields. *Journal of Hydrology* **248**: 1–13.

USDA-SCS. 1986. *Urban Hydrology for Small Watersheds*, Technical Release 55. Washington, DC.

Van Oost K. 2003. *Spatial Modelling of Soil Redistribution Processes in Agricultural Landscapes*, PhD thesis, K.U. Leuven.

Van Oost K, Beuselinck L, Hairsine PB, Govers G. 2004. Spatial evaluation of multi-class sediment transport and deposition model. *Earth Surface Processes and Landforms* **29**: 1027–1044.

Van Oost K, Govers G, Desmet P. 2000. Evaluating the effects of changes in landscape structure on soil erosion by water and tillage. *Landscape Ecology* **15**: 577–589.

Verstraeten G, Poesen J. 1999. The nature of small-scale flooding, muddy floods and retention pond sedimentation in central Belgium. *Geomorphology* **29**: 275–292.

Williams JR, Renard KG. 1985. Assessments of soil erosion and crop productivity with process models (EPIC). In *Soil erosion and crop productivity*, Follett RF, Stewart BA (eds). American Society of Agronomy, Wisconsin, USA; 63–103.

Wischmeier WH, Smith DD. 1958. Rainfall energy and its relationship to soil loss. *Transactions of the American Geophysical Union* **39**: 285–291.

Wischmeier WH, Smith DD. 1978. *Predicting Rainfall Erosion Losses – a Guide to Conservation Planning*. U.S. Government Print Office, Washington, USA.